# Investigation of Nano- and Micro-Sized Amorphous Materials under the Influence of High-Energy Radiation

Mohammed M. Sabri

Department of Physics, Faculty of Science and Health, Koya University,
Koya KOY45, Kurdistan Region - F.R. Iraq

***Abstract*—This research explored the behavior of glass when bombarded by high-energy radiation, especially electron beams inside transmission electron microscopy (TEM). Six types of glasses are investigated under e-beam. The work is conducted using three types of TEMs of energies of 120, 200, and 300 keV. The findings show that these microscopies have a significant impact on the glass, as various observations were documented. Using a wide electron beam, morphology changes combined with bubble formation are observed in the glass. These changes are rounding and smoothening of glass edges and surfaces. In addition, the findings show that there is no material loss due to irradiation as confirmed by the energy dispersive X-ray spectroscopy. The results also show that high silica glass is very sensitive, while high boron glass is found to be less sensitive to irradiation. Using a smaller size electron beam, on the other hand, resulted in the fabrication of a nanoring/nanocrater in glass. The possible applications of this research can be in the protection and packaging of three-dimensional electronic equipment and nanoscale pattern formation through roughening of the external glass contour through phase separation and the opposite through local changing of a part of the glass through the pseudo-melting and the stability of loaded and un-loaded glasses to the irradiation. Furthermore, by generating a nanoring or a nanocrater through e-beam, the lithography process is successfully performed, as the effect of the electron beam is solely at the irradiation region, while the regions outside the e-beam remain unaffected.**

***Index Terms*—Glass, Morphology changes, Nanoring, Quasi melting, Transmission electron microscopy.**

## I. Introduction

Irradiation with high-energy radiation has been reported to perform changes in nano and micro-size amorphous materials, especially glass (Jiang, et al., 2004; Singh and Karmakar, 2011; Ehrt and Vogel, 1992; Sidorov, et al., 2021). This topic has become of great interest and, therefore, attracted a variety of researchers in the past and recently (Shelby, 1980; Abo Hussein, 2023). This is due to the fact that radiation has an important impression on the structures, characteristics, morphologies, and compositions of these materials. A variety of changes have been reported to occur when the e-beam interacts with a material (Hobbs, 1987; Chen, et al., 2021). Various definitions have been reported on glass (Mauro, et al., 2013), focusing either on its physical properties or on its structure. Usually, all glasses were found to share two common properties. These are as follows: (i) glass has a short-range order of the atomic arrangement and (ii) glass has a behavior of time-dependent glass transformation (Guigo and Sbirrazzuoli, 2018; Shelby, 2005). The American Society for Testing and Materials defines glass as "an inorganic product of fusion which has cooled to a rigid condition without crystallization." A typical type of glass is oxide glass. These glasses are considered to be prototype brittle materials that became significant member of nowadays nano and micro components in terms of structure and function (Bruns, et al., 2023). Usually, three fundamental types of oxides are available. Glass formers such as silica and boric oxide, glass modifiers such as soda and lithium oxide, and intermediates such as $Al_2O_3$. Changes due to radiation of glass with a high-energy particle include for instance the modifications in the external shapes of the glass, in particular, changing the external parts of the glass fragment (Gedeon, et al., 2007; Zheng, et al., 2010) and other amorphous materials (Shen, et al., 2022), phase separation (Chen, et al., 2015; DeNatale, et al., 1986; Sun, et al., 2004), ion migration (Yoshida and Tanaka, 1997; Jbara, et al., 1995; Gedeon, et al., 1999), phase alteration (Liu, et al., 2004), the production of bubbles (Leay and Harrison, 2019), which was considered to be oxygen, nanoprecipitation (Qiu, et al., 2002), crystallization (Klimenkov, et al., 2001; Jencic, et al., 1995), hole drilling (Furuya, 2008), and quasi-melting (Ajayan and Ijima, 1992; Ajayan and Marks, 1989; Marks, et al., 1986). Most of these changes were frequently reported in oxide glasses (Skuja, et al., 2005), while the phenomenon of shape transformations was rarely reported (Li, et al., 2019). The latter was sometimes noticed accidentally, while sometimes deliberately studied. Transmission electron microscopy (TEM) is a widely used technique and considered to be a powerful tool for irradiation-induced modifications, formation of nanoparticles, and also for the purpose of recording images (Duan, et al., 2018; Sigle, 2005; Egerton et al., 2004). Moreover, exploring electron beam-materials interaction is of a great interest

ARO-The Scientific Journal of Koya University
Vol. XI, No. 2 (2023), Article ID: ARO.11290, 10 pages
DOI: 10.14500/aro.11290
Received: 27 July 2023; Accepted: 09 September 2023
Regular research paper: Published: 24 September 2023
Corresponding author's e-mail: mohammed.mohammedsabri@koyauniversity.org
Copyright © 2023 Mohammed M. Sabri. This is an open access article distributed under the Creative Commons Attribution License.

http://dx.doi.org/10.14500/aro.11290

(Dapor, 2003). Normally, scattering of both types elastic and inelastic is reported to occur when an e-beam hits a material, and this will be the source of giving essential knowledge on the structure and the composition of the sample. One of the significant importance of using a transmission electron microscope is to modify the amorphous materials and can track these modifications *in situ* (live) and this will allow the discovery of novel phenomena such as nanoscale and microscale phase changes and morphology changes in these materials (Rauf, 2008; Mackovic, et al., 2014; Butler, 1979). Usually, three various mechanisms are involved in the interaction of a high-energy radiation with materials. These are as follows: (i) ionization and electronic excitation processes through radiolysis (Ugurlu, et al., 2011), (ii) direct displacement of the atoms by fast high-energy radiation (elastic collisions) through knock-on (Ugurlu, et al., 2011), and (iii) heating (Liu, et al., 1994; Sidorov, et al., 2021). The first mechanism, on the one hand, involves damage to the electronic structure and bond breakage, which may lead to the displacement of atoms as a secondary effect converting excitonic energies generated during incident probe-atomic electron interactions into momentum by forming a Frenkel pair. The second mechanism, on the other hand, includes direct atom displacement, which may be followed by rearrangement of the electronic structure. Finally, under a high-energy radiation, the specimen will be saturated with energy through electron-phonon scattering and this will cause the specimen to be heated. It has been suggested that the quality of the heat flow connection to the sample support may affect the temperature alteration from a few degrees up to melting (Hobbs, 1987; Bysakh, et al., 2004). The effects of heating in the TEM can be minimized using several methods such as avoid the usage of thick samples and using thin sample instead, coating the sample with conducting materials, and using unheated holders.

The main purpose of the current research is to explore the influence of irradiation by the electron beam on different glasses and then explain the resulting phenomena that occurred in these materials.

## II. Materials And Methods

The experimental procedure consists of three main stages. These stages are as follows: (i) glass preparation through typical melting process, (ii) TEM sample preparation, and (iii) the irradiation process. All the micrographs that obtained from the irradiation process were analyzed using image J software (Image J Launcher version 1.4.3.67 with an accuracy of about 100%). This software was used to determine the radius of curvature of the rounded corners of the glass fragments, to determine the size of the nanoparticles, as well as to determine the size of the nanorings.

### *A. Producing the Glass through Melting Process*

The initial step of the glass preparation is mixing the raw materials manually and then weight about 300 g of each glass batch for the melting process. All raw materials were oxides and carbonates ($Na_2CO_3$, $H_3BO_3$, $SiO_2$, $CaCO_3$, $Al_2O_3$, $Li_2O$, $CeO_2$, $Cr_2O_3$, and $ZrO_2$) and they were all purchased from the company Sigma-Aldrich and their purity of about 99.9%. The batch was, then, transferred to the platinum crucible (of a cylindrical shape having a height of about 12 cm and base diameter of about 5 cm), and the latter was transferred to the electric furnace of an internal volume of about 148 $cm^3$ with silicon carbide elements for the purpose of melting. The entire melting process lasted 5 h. After that, about 20% of the product was fast-cooled (quenching process) in water to get a quenched glass and the rest (~ 80%) was transferred to another furnace for slow cooling (annealing process) to get an annealed glass. The degree of annealing temperature was 510°C for 1 h. Six different glasses were used. One of them is a silica-free (Si-free) glass and named as NB. The second glass is a high-Si glass and named as NBS-HS and the third is a high-B glass and named as NBS-HB. The fourth is a boron-free (B-free) glass and named as NCS. The fifth glass contains both Al and Ca and named as ACBS. The last glass is alkali-mixed glass and named as AMBS. Table I shows the chemical composition of the prepared glass along with the melting temperature of each glass.

### *B. Sample Preparation for TEM Tests*

TEM specimens were prepared by manually grinding the quenched glass into a very fine powder (the amount of the powder used was about 20–30 g) in acetone using a pestle and mortar. The mixture (powder and acetone) was, then, transferred to the ultrasonic machine and was left for about 15 min to decrease or remove the amount of the agglomeration. A fresh TEM sample holder (either gold or copper grids with carbon film) was, then, carried by tweezers and immersed into the mixture to pick up the glass. Finally, the TEM sample is transferred to the microscope for the irradiation study.

### *C. e-beam Irradiation Procedure*

Three different types of TEMs were used to conduct the irradiation. First, TEM of type Philips 420 thermionic tungsten at 120 kV is used to investigate the effect of the electron beam in modifying the shape of the glass fragment. The captured images in this microscope were saved in photographic plates and, then, collected and scanned using a normal scanning machine to get the final micrographs. Normally, the irradiation

TABLE I
The chemical composition (mol. %) Of the glass and the melting temperature (oc)

| Glass name | Glass code | Glass composition | Melting temperature |
|---|---|---|---|
| Silica-free | NB | $21.16Na_2O$-$70.84B_2O_3$-$4CeO_2$-$2Cr_2O_3$-$4ZrO_2$ | 1250 |
| High silica | NBS-HS | $16.6Na_2O$-$20B_2O_3$-$63.4SiO_2$ | 1200 |
| High boron | NBS-HB | $16.6Na_2O$-$62.55B_2O_3$-$20.85SiO_2$ | 1100 |
| Boron-free | NCS | $18.3Na_2O$-$18.3CaO$-$63.4SiO_2$ | 1450 |
| Al-Ca glass | ACBS | $8Al_2O_3$-$27CaO$-$8B2O3$-$57SiO_2$ | 1450 |
| Alkali-mixed glass | AMBS | $8.6Na_2O$-$4.3Li_2O$-$25.7B_2O_3$-$51.4SiO_2$-$4CeO_2$-$2Cr_2O_3$-$4ZrO_2$ | 1400 |

process in this TEM has been conducted using the largest condenser aperture and spot size 1. Second, TEM of type JEOL JEM 2010F field emission gun (FEG) at 200 kV, which has the capability of getting a finer electron beam (few nm in size) than that in the TEM of type Philips 420 and also provides a charged coupled device (CCD) camera to take digital images and third, TEM of type JEOL JEM 3010 lanthanum hexaborides ($LaB_6$) of a voltage of 300 kV. In this microscope, a higher current is available and this allows to irradiate of the samples with a higher accelerating voltage in comparison to the TEM 2010F at 200 kV and TEM 420 at 120 kV. However, the e-beam cannot be focused on that much compared to TEM 2010F (FEGTEM) due to the filament source of the former TEM. There is also a CCD camera in this TEM to record the images. It is worth mentioning that all the three TEMs used in this research are located at the University of Sheffield-United Kingdom. Fig. 1 illustrates a schematic diagram of the mechanisms used in this research. These include (i) morphology alteration experiments, (ii) hole drilling, and (iii) imaging.

## III. Results And Discussion

### *A. Shape Alteration Due to e-beam Irradiation*

It has been proven that an electron beam is a versatile tool for performing alterations into glass (Musterman, et al., 2022). In addition, *in situ* TEM is most widely used technique due to its various characteristics, and due to the fact that *in situ* TEM is enthusiastic by observing the real-time material modification, the effect of the e-beam cannot be neglected (Shen, et al., 2022). The experiment of shape alteration has been performed by reducing the diameter of the e-beam in such a way that covering the entire glass fragment. The e-beam is then will be leaving at this condition for a selected period of time and monitoring the live morphology changes. When the irradiation process is completed, a micrograph of the irradiated glass fragment at a selected magnification will be captured. Fig. 2 shows a sample of the alkali-mixed glass before and subsequent 5 min of electron irradiation. This glass sample is of sharp corners and coarse edges, as shown in Fig. 2a. Our measurements of this fragment before the irradiation were as follows: position 1, position 2, and position 3 have a radius of curvature of about 4 nm, 7 nm, and 7.5 nm, respectively. The e-beam diameter has then been reduced to cover the whole glass particle (the size of the electron beam ~ 500 nm). After about less than a minute of irradiation, the modifications were initiated. These modifications are smoothening of the rough surfaces and edges and rounding of the sharp corners, as shown in Fig. 2b. From Fig. 2b, it is clear that the morphology of the entire glass sample was altered and if the irradiation process continued for a longer time, the glass particle in Fig. 2a might be gotten more rounded to form a full ball-shape. The measurements after the entire 5 min of irradiation, however, were as follows: the radius of curvature of position 1 is about 5 nm, the radius of curvature of position 2 is about 26 nm, and the radius of curvature of position 3 is about 16 nm. The impacts of the e-beam on the glass fragment are obvious through noticing the shape-changing. The electron beam is wide enough to cover the entire glass fragment (the size of the electron beam is larger than the size of the glass fragment) and the first part subjecting to the alteration is the corner of the glass sample. Usually, the flow of materials due to e-beam irradiation was reported to be the reason for the phenomenon of morphology alteration in glass (Bruns, et al., 2023).

Now, a sample of a high-Si glass has been irradiated for 5 min. After ~ 1 min of e-beam irradiation, this sample underwent a morphology modification. This glass sample is some sharp corners (positions 1 and 2 in Fig. 3a). These positions became rounded after the irradiation (the same positions shown in Fig. 3b). This is again proposed to be due to the movement of glass material (Bruns, et al., 2023). As such, the material will be moved into the middle of the glass fragment and accumulate there and therefore this fragment looks darker after irradiation (Fig. 3b). In addition, a little

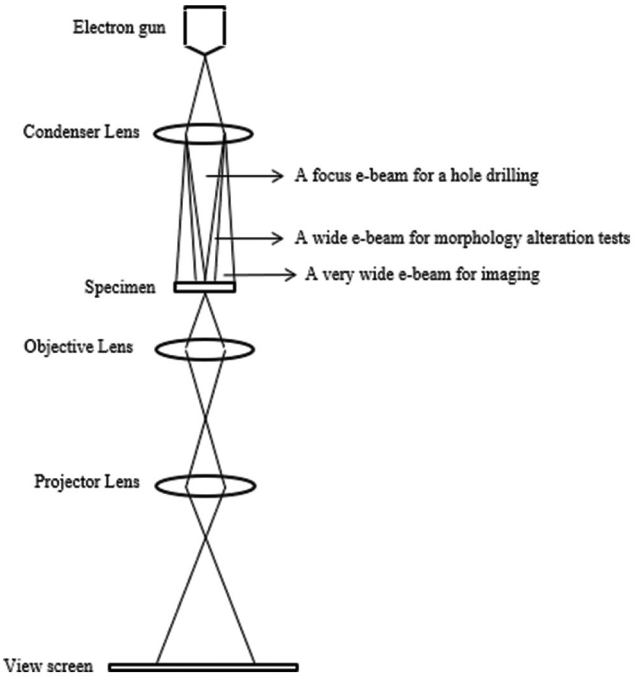


Fig. 1. A schematic diagram showing the three mechanisms used in the transmission electron microscopy.

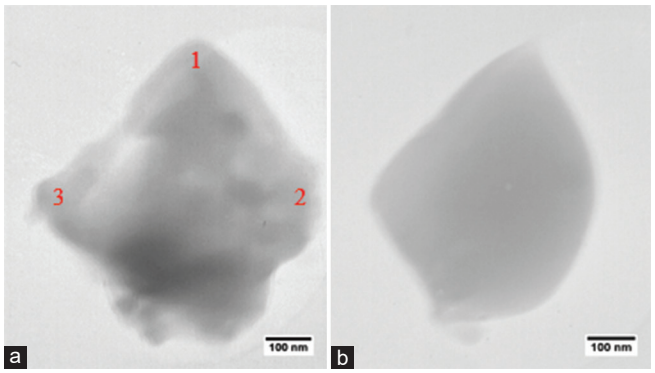


Fig. 2. An alkali-mixed glass (a) at t=0 min and (b) at t=5 min irradiation using a transmission electron microscopy of type Philips 420 at 120 kV.

http://dx.doi.org/10.14500/aro.11290

smoothing effect on the bottom part of this fragment can be seen due to the irradiation. Our experiments showed that before the irradiation, the radius of curvatures of position 1 and position 2 was 5 nm and 6 nm, respectively (as shown in Fig. 3a). However, after 5 min of irradiation, the radius of curvatures of position 1 and position 2 dramatically increased to about 15 nm and 8 nm, respectively (Fig. 3b). This result is consistent with the results reported by Singh and Karmakar in which they observed morphological alterations (rounding of glass edges) of glass fragment in bismuth-doped oxide glass (Singh and Karmakar, 2011). In addition, the results observed in this research are agreed with what have been reported by Jiang and his group in terms of smoothing of the rough glass surface in germanium glass (Jiang, et al., 2005).

The chemical composition of this glass was explored before and after the irradiation using energy-dispersive X-ray spectroscopy (EDX), as shown in Fig. 4. Both spectra contain the glass elements of oxygen, sodium, silicon, and boron. It is obvious that before (Fig. 4a) and after irradiation (Fig. 4b), there is no difference in the composition of this fragment and this gives an indication and confirmation of no loss of materials occurred due to the e-beam irradiation. Furthermore, the copper (Cu) peaks (signals) that appeared in the energy dispersive spectroscopy spectra are belonging to the copper grid used to hold the glass specimen for TEM measurements.

A time-series irradiation of a fragment of the B-free glass has been performed, as shown in Fig. 5. Usually, time-series is an important process in the field of e-beam-induced modifications in glass. This process gives a chance to live observe and track the alteration of the irradiated glass sample. Fig. 5a shows a fragment of the B-free glass at t = 0 min. When this glass was irradiated for about 1-min, a slight alteration can be evident, as shown in Fig. 5b. These alterations were not stopped when the glass sample was irradiated for extra 2 min and 5 min, as shown in Figs. 5c and d, respectively. All these alterations occurred to this sample are in terms of rounding of the corners as well as smoothening of the coarse surfaces (Singh and Karmakar, 2011; Jiang, et al., 2005).

A sample of the Si-free glass has been shown to be robust under irradiation, as shown in Fig. 6. This sample was analyzed using a JEOL 2010F TEM. The total irradiation process was 5 min. A slight modification in this glass fragment was noticed, in which the bottom corner of the fragment shown in Fig. 6a underwent a slight rounding when subjected to the irradiation (Fig. 6b). This is due to the fact that this glass showed its robustness to the irradiation (Jiang, et al., 2023). In addition, the coarse edges of this fragment became smooth.

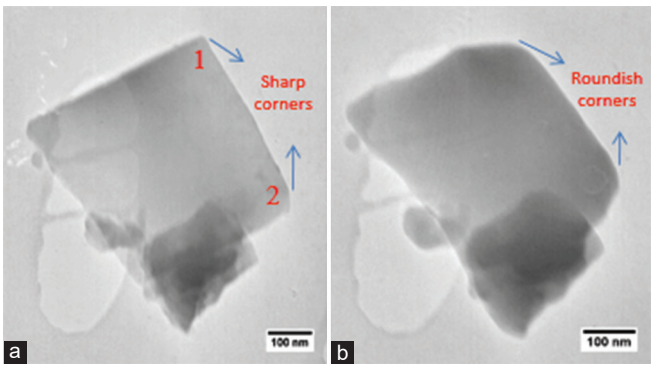


Fig. 3. A high-Si glass before (a) and after 5 min irradiation (b) using a transmission electron microscopy of type Philips 420 at 120 kV

The spectrum shown in Fig. 7 is a point EDX spectrum of the high-B glass. The significance of these spectra is that it is obvious that there was a substantial decrease in the amount of boron. Furthermore, the amount of sodium was decreased from about 9.74% before the irradiation to about 3.20% due to subsequent irradiation. This effect is believed to be due to alkali migration under irradiation (Sidorov, et al., 2021; Hofmann, et al., 2023). However, the alteration of O and Si is not significant. In addition, the gold (Au) peaks (signals) appeared in the EDX spectra are belonging to the gold grid used to hold the glass specimen for the TEM measurements.

A sample of the AL-Ca glass was also time-series investigated under the e-beam, as shown in Fig. 8. Significant shape transformations were observed. The 300 kV e-beam irradiation was enough to perform these changes and also influenced the carbon film as can be seen in the left side of Fig. 8d-f. It was observed that increasing the irradiation time resulted in smoothening the rough edges and surfaces of the glass fragment. In addition, the rounding of the glass fragment's corners was increased with increasing the irradiation time. For example, the lower right corner of the glass fragment has the data tabulated in Table II below.

A thick B-free glass particle of about 500 nm in size has been explored under the influence of the irradiation, as seen in Fig. 9 using a time-series technique to track the changes that occurred with increasing the irradiation time. Obviously, from t = 0 min (Fig. 9a) to t = 6 min irradiation (Fig. 9g), substantial morphology transformations occurred due to the large amount of energy delivered by the e-beam (300 keV). The glass fragment gradually changed its shape into almost a sphere shape and all rough edges and surfaces became smooth on increasing the irradiation time.

Another phenomenon that can be occurred as a result of electron beam irradiation and is believed to be associated with the morphology alteration is bubble formation (Weber, et al., 1997). Fig. 10 represents a B-free glass irradiated between t = 1 min to t = 5 min. The sample shown in Fig. 10a is clean with free of any bubbles. However, after the irradiation was initiated, the bubble started to form and the number of bubbles increased with increasing the irradiation time (For example Fig. 10b and Fig. 10c). In Fig. 10d, it seems that at 3 min irradiation, the bubbles were merged producing larger bubbles. This was continued by increasing the irradiation time in which at t = 5 min, all bubbles were merged

TABLE II
THE AMOUNT OF ROUNDING OF A CORNER OF THE GLASS FRAGMENT

| Irradiation time (min) | The amount of rounding (nm) |
|---|---|
| 0 | 30 |
| 1 | 45 |
| 2 | 50 |
| 3 | 65 |
| 4 | 90 |
| 5 | 110 |

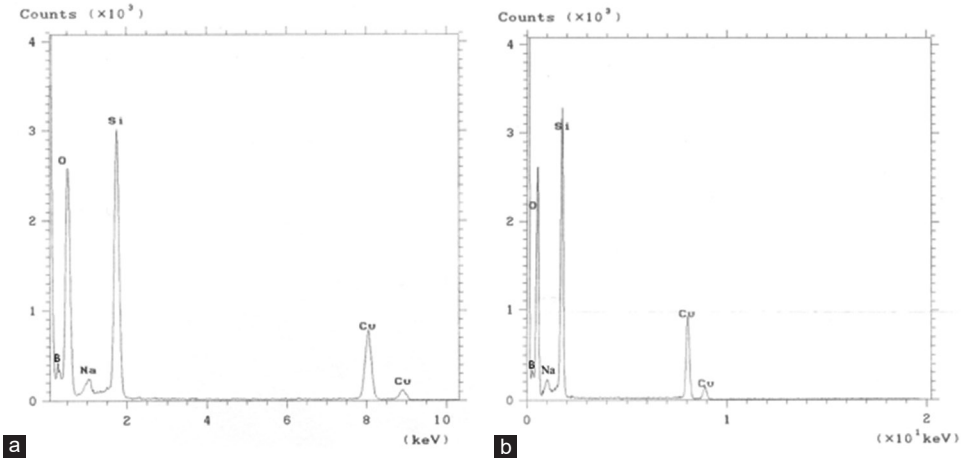


Fig. 4. Energy dispersive x-ray spectroscopy spectra of the high-Si glass before (a) and after irradiation (b).

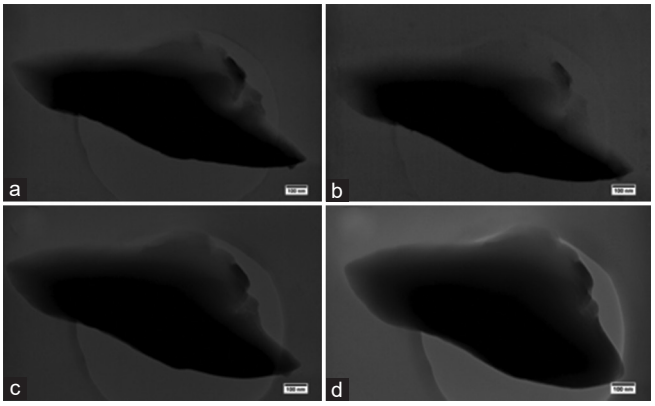


Fig. 5. A time-series irradiation of the B-free glass at (a) no irradiation, (b) 1 min, (c) 2 min and (d) 5 min using a transmission electron microscopy of type Philips 420 at 120 kV.

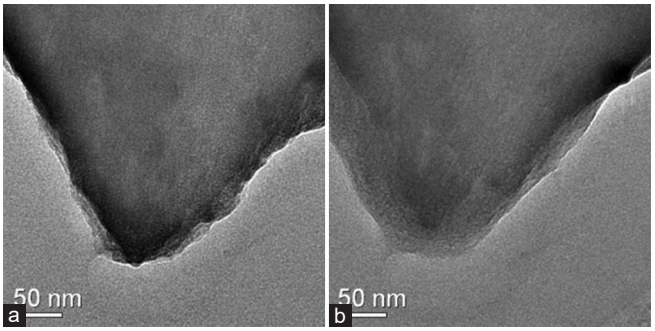


Fig. 6. A slight modification in a Si-free sample using transmission electron microscopy JEOL JEM 2010F at 200 kV. (a) before irradiation and (b) after 5 min irradiation.

and only a few were left. Moreover, the other effects of the irradiation that can be seen are rounding of the entire fragment and smoothening of the coarse surfaces. It seems that bubble formation is a secondary effect associated with the morphology alteration phenomenon. This is a beneficial to understand the mechanism of this phenomenon, as it is obviously very difficult to be produced by temperature, but rather the kinetic activation role in which the fast electrons play at a temperature well below the melting point (Ollier, et al., 2006; Leay and Harrison, 2019).

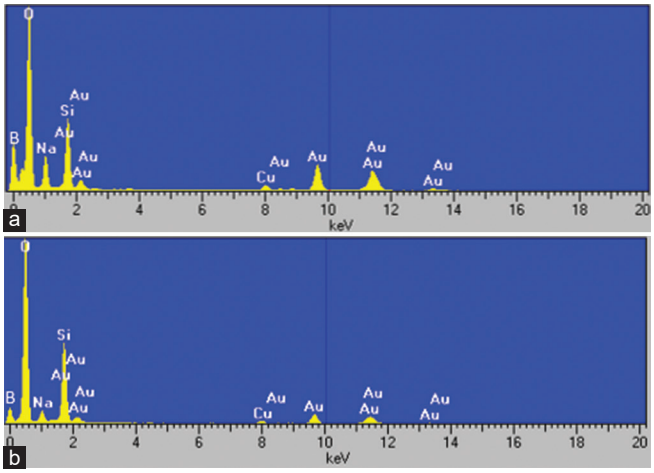


Fig. 7. The electron dispersive x-ray spectroscopy spectrum for the fragment of the high-B glass (a) without e-beam irradiation and (b) subsequent irradiation.

To confirm the robustness of a high-B glass, a fragment of this glass was inserted into the TEM of type JEOL JEM 3010 at 300 kV and irradiated for 1 and 2 min, respectively, as shown in Fig. 11. Before the irradiation, the fragment was of a rough edge as indicated by the red arrows in Fig. 11a. However, this rough edge has been smoothened and the roughness partially disappeared after 1 min of irradiation as indicated by the yellow arrows in Fig. 11b and continued to be smoothened at 2 min of irradiation, and now, there is no any trace of roughness and the entire edge became smooth, as shown in Fig. 11c. As a combined phenomenon of morphology alteration, a few bubbles were also formed as denoted by the green arrows in Fig. 11c.

This glass was also imaged using scanning electron microscopy (SEM) of type JEOL JEM 6400 combined with an EDX, as shown in Fig. 12.

### *B. Fabrication of Nanostructures (Nanoring/Nanocrater) Using Electron Beam*

It has been reported that an electron beam in TEM is a versatile tool to produce nanostructures including rings, crater,

http://dx.doi.org/10.14500/aro.11290

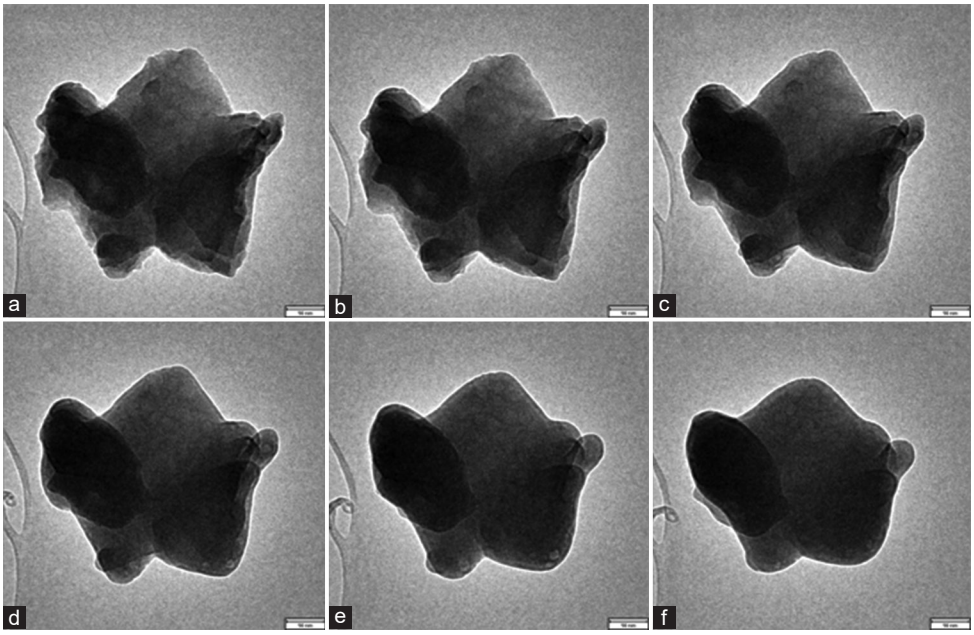


Fig. 8. A time-series irradiation of a fragment of the AL-Ca glass at (a) 0 min, (b) 1 min, (c) 2 min, (d) 3 min, (e) 4 min and (f) 5 min using a transmission electron microscopy of type JEOL JEM 3010 at 300 kV and showing significant shape alterations. The scale bar in all images is 90 nm.

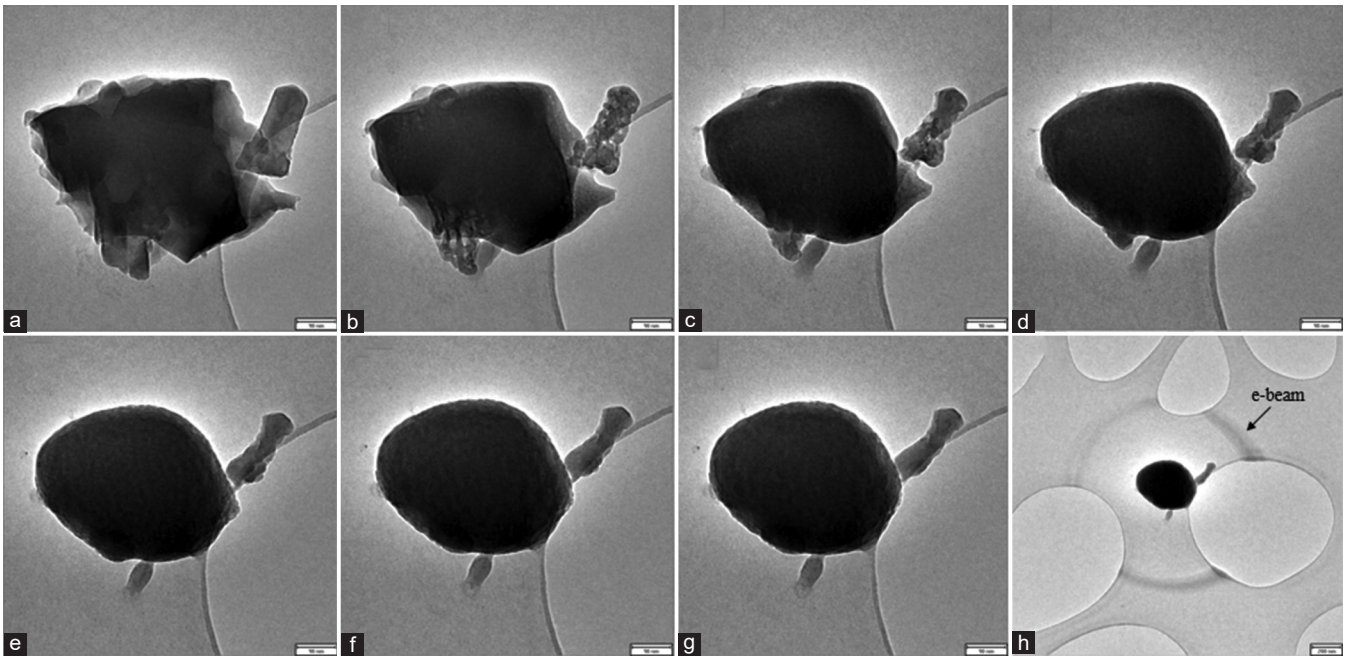


Fig. 9. A time-series irradiation of a fragment of the B-free glass at (a) t = 0-min, (b) t = 1 min, (c) t = 2 min, (d) t = 3 min, (e) t = 4 min, (f) t = 5 min and (g) t = 6 min irradiation using a transmission electron microscopy of type JEOL JEM 3010 at 300 kV. (h) is a higher magnification micrograph of (g) showing the diameter of the e-beam. The scale bar in (a-g) is 90 nm and in (h) is 200 nm.

and nanoparticles (Martinez, et al., 2016). An experiment has been performed to produce a hole (ring) in the glass using a TEM of type JEOL JEM 3010 at 300 kV, as shown in Fig. 13. Hole drilling through e-beam has been discussed as achieving very localized melting and ablation by evaporation even in metals on well-conductive support as a result of kinetic heat transport delays (Bysakh, et al., 2004). In Fig. 13a and b, a hole of a diameter of about 100 nm in the high-B glass and a hole of a diameter of about 100 nm in the high-Si glass have been successfully fabricated, respectively. Usually, holes and rings are considered to be 2D structures in which their thickness is much smaller than their diameter (Jiang, et al., 2003). Moreover, rings fabrication in glasses by electron irradiation was believed to be due to the ionization and migration process. Our difficulties in the process of producing a hole in the glass is that live observation for tracking such a process from the beginning to the end is somewhat impossible due to the extremely high e-beam intensity when focusing on a spot and a 300 kV electron beam is enough to give an extremely high intensity. Therefore, the e-beam will

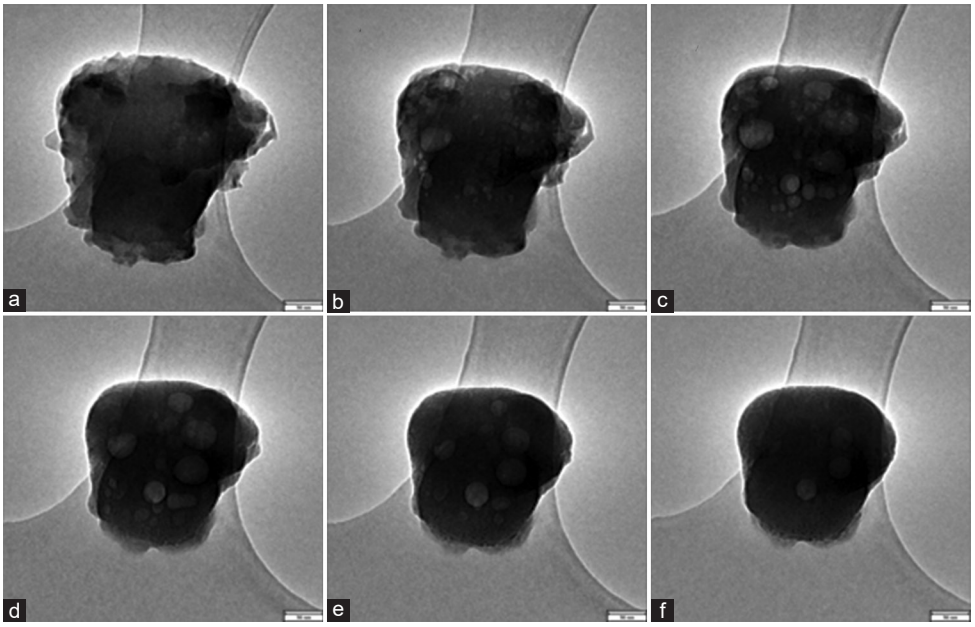


Fig. 10. A boron-free glass (a) at t = 0 min and (b-f) at t = 1 to t = 5 min irradiation using a transmission electron microscopy of type JEOL JEM 3010 at 300 kV. The scale bar in all images is 90 nm.

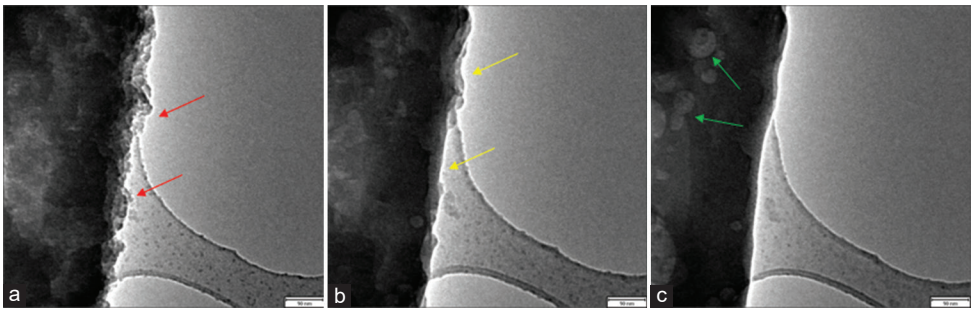


Fig. 11. A high-B glass (a) at t = 0 min, (b) at t = 1 and (c) at t = 2 min irradiation using a transmission electron microscopy of type JEOL JEM 3010 at 300 kV. The scale bar in all images is 90 nm. The red and yellow arrows represent the roughness versus the smoothness of the fragment edge at t = 0 min and t = 1 min, respectively. The green arrows represent the bubbles formed as a result of e-beam irradiation.

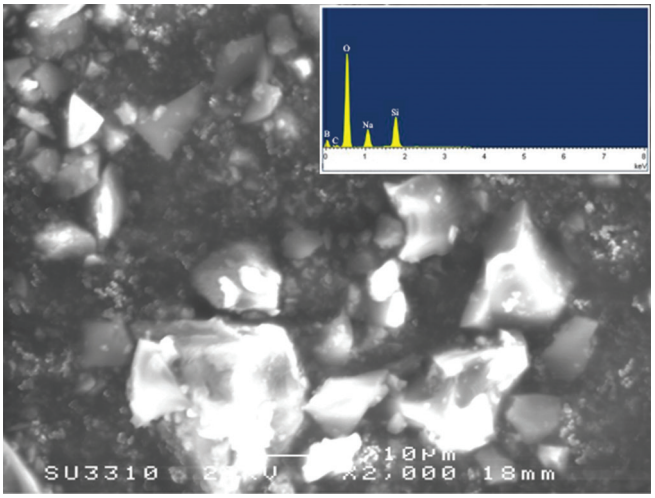


Fig. 12. A secondary electron image of a high-B glass using SEM of type JEOL JEM 6400. The inset is the EDX spectrum of the fragment.

be focused to fabricate the hole, and then, the e-beam will be spread to photograph the hole. The process in Fig. 13c is somewhat different and can be named a crater formation rather than a hole (ring) formation. This is due to the fact that in the crater formation, many tiny spherical-shaped nanoparticles of the size of about 15 nm were formed inside and around the electron beam (the yellow square shape in Fig. 13c), which are believed to be one of the loaded elements in this glass (alkali-mixed), that is, cerium, chromium, or zirconium. It has been demonstrated that the electron beam irradiation increased the atom diffusion by several orders of magnitude compared to that in thermal treatment. The fabrication of nanoparticles occurs at both distinctly lower temperature and significantly higher rates of the irradiation. This explains that the electron beam irradiation can result in a fast grain growth of the primary nucleated nanoparticles leading to bigger smallest-sized particles (Ahn et al., 2015). Furthermore, A possible explanation for crater fabrication by the electron beam is the alkali migration (Gedeon, et al., 1999), as the two alkalis contained in this glass are Na and Li and they are both positive ions; hence, they migrate away from the negativity charged electron beam. It is believed that a highly focused electron beam (the intensity of about 180 pA/cm$^2$) dominantly contributes to the sputtering effect (such as in Fig. 13a and

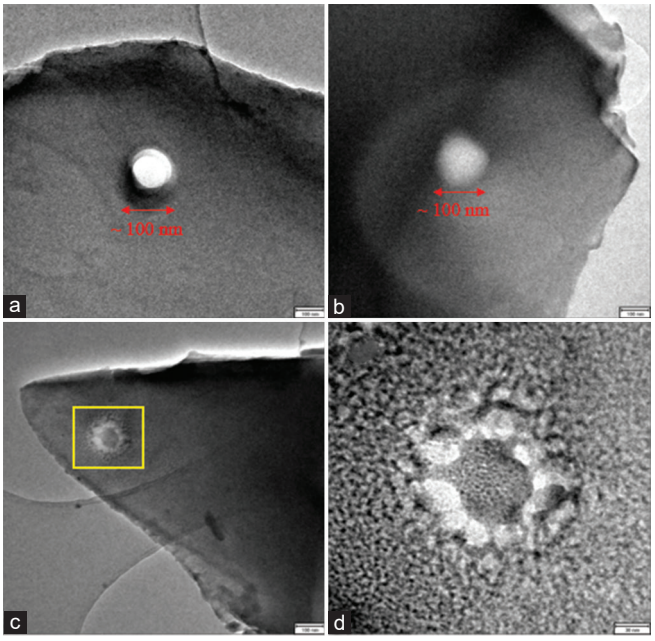


Fig. 13. The effect of a fully focused electron beam on (a) high-B glass, (b) high-Si glass, (c) alkali-mixed glass using a transmission electron microscopy of type JEOL JEM 3010 at 300 kV. (d) is a magnified micrograph of the irradiated area in (c) (the yellow square shape). The scale bar in (a-c) is 100 nm and in (d) is 30 nm.

b), while a slightly spread e-beam (the intensity of about 130 pA/cm$^2$) mostly contributes to the diffusion of the atoms forming nanoparticles (such as in Fig. 13c and d).

In general, the speed of shape changes including rounding of the sharp corners and smoothening and flattening of the rough edges and surfaces is faster in TEM of type JEOL JEM 3010 at 300 kV and in TEM of type JEOL JEM 2010F at 200 kV than in TEM of type Philips 420 at 120 kV. This is true because the higher voltage TEM has the higher energy, and hence, the alteration that occurred in the irradiated glass will be faster. Usually, the phenomenon of shape transformation was believed to be due to the reduction of the surface energy anisotropy as the temperature is raised, that is, either the thermal or the electronic temperature. Through the *in situ* observations, the speed of glass rounding and flattening was faster in the high-Si glass and slower in the high-B glass. This is due to the relationship between this effect and the melting temperature ($T_m$) and the glass transition temperature ($T_g$) of those glasses and some other amorphous materials (Rao, et al., 2021; Mohammad, et al., 2016). Therefore, it can be supposed that the high-B glass is a robust glass under the influence of the electron beam. It has been reported that the migration of $Na^+$ increases with reducing the percentage of $B_2O_3$ (We, et al., 2011). This is applicable to what has been found in this research, as the morphology alteration of glass were substantial in the high-Si glass, while these alterations were slight in the high-B glass due to the strongly bonded of Na and B in the glass network. It has also been proposed that the greatest significant technique for the movement of the glass material due to the radiation was the formation of point defects (Mayr, et al., 2003). Usually, glasses are sensitive to irradiation because they are not in the thermodynamic minimum and hence the glass under irradiation can be readily altered (Gedeon, et al., 2007). Nanoring and crater formation, on the other hand, show the capability of electron beam in tailoring the glass material, especially in the fabrication of these structures. The fabrication of nanorings and nano-crater in glasses by the electron beam is believed to be a result of ionization and field-induced migration (Furuya, 2008). In addition, a changeable local structure in the medium range is existing in the amorphous materials and this permits fabricating rings with desired properties (Jiang, et al., 2003).

## IV. Conclusion

The influence of high-energy radiation in different glasses has been investigated using three different types of TEMs. It has been concluded that irradiation through the electron beam has a considerable impact on the glasses. In this research, morphology alterations of the glasses were observed through the phenomenon of rounding the sharp corners and smoothening the rough edges and surfaces of the glass sample. It was also concluded that the radius of curvature (the amount of glass corner's rounding) increased when the irradiation time increased. Bubble formation, on the other hand, was observed as a combined effect with e-beam-induced morphology alteration, which was believed to be oxygen, and no materials loss was observed due to the irradiation. Moreover, nanoring and nanocrater fabrication in the glasses were successfully performed.

## V. Acknowledgment

The author thanks and acknowledges Koya University, Faculty of Science and Health, Department of Physics for enabling this work as well as Dr. Guenter Moebus and Dr. Guang Yang for their help.

## References

Abo Hussein, E.M., 2023. The impact of electron beam irradiation on some novel borate glasses doped $V_2O_5$; Optical, physical and spectral investigation. *Inorganic Chemistry Communications*, 147, pp.110232.

Ahn, J.H., Eom, J.Y., Kim, J.H., Kim, H.W., Lee, B.C., and Kim, S.S., 2015. Synthesis of $TiO_2$ nanoparticles induced by electron beam irradiation and their electrochemical performance as anode materials for Li-ion batteries. *Journal of Electrochemical Science and Technology*, 6(3), pp.75-80.

Ajayan, P.M., and Ijima, S., 1992. Electron irradiation-induced dynamical fluctuations in amorphous structures. *Journal of Non-Crystalline Solids*, 150, pp.423-428.

Ajayan, P.M., and Marks, L.D., 1989. Experimental evidence for quasi melting in small particles. *Physical Review Letters*, 63(3), pp.279-282.

Bruns, S., Minnert, C., Petho, L., Michler, J., and Durst, K., 2023. Room temperature viscous flow of amorphous silica induced by electron beam irradiation. *Advanced Science*, 10, pp.2205237.

Butler, E.P., 1979. *In situ* experiments in the transmission electron microscope. *Reports on Progress in Physics*, 42, pp.834-889.

Bysakh, S., Shimojo, M., Mitsuishi, K., and Furuya, K., 2004. Mechanisms of nano-hole drilling dye to nano-probe intense electron beam irradiation on a

stainless steel. *Journal of Vacuum Science and Technology B*, 22(6), pp.2620-2627.

Chen, L.T., Ren, X.T., Mao, Y.N., Mao, J.J., Zhang, X.Y., Wang, T.T., Sun, M.L., Wang, T.S., Smedskjaer, M.M., and Peng, H.B., 2021. Radiation effects on structure and mechanical properties of borosilicate glasses. *Journal of Nuclear Materials*, 552, pp.153025.

Chen, X.Y., Zhang, S.G., Xia, M.X., and Li, J.G., 2015. Phase separation and crystallization induced by electron irradiation in nanoscale $Fe_{56.5}Mn_{11}Cr_{8.5}Ni_4Si_{10}C_{10}$ metallic glass. *Acta Metallurgica Sinica*, 28, pp.1332-1335.

Dapor, M., 2013. *Electron-beam Interactions with Solids*. Vol. 186. Springer, Berlin, Heidelberg, pp.1-110.

DeNatale, J.F., Howitt, D.G., and Arnold, G.W., 1986. Radiation damage in Silicate glass. *Radiation Effects*, 98, pp.63-70.

Duan, B.H., Chen, L., Lv, P., Du, X., Zhang, L.M., and Wang, T.S., 2018. *In situ* TEM study on electron irradiation effect in $SiO_2$-$Na_2O$-$B_2O_3$ glasses. *International Journal of Applied Glass Science*, 10(2), pp.220-227.

Egerton, R.F., Li, P., and Malac, M., 2004. Radiation damage in the TEM and SEM. *Micron*, 35, pp.399-409.

Ehrt, D., and Vogel, W., 1992. Radiation effects in glasses. *Nuclear Instruments and Methods in Physics Research Section B: Beam Interactions with Materials and Atoms*, 65, pp.1-8.

Furuya, K., 2008. Nanofabrication by advanced electron microscopy using intense and focused beam. *Science and Technology of Advanced Materials*, 9, pp.014110.

Gedeon, O., Jurek, K., and Drbohlav, I., 2007. Changes in surface morphology of silicate glass induced by fast electron irradiation. *Journal of Non-Crystalline Solids*, 353, pp.1946-1950.

Gedeon, O., Jurek, K., and Hulinsky, V., 1999. Fast migration of alkali ions in glass irradiated by electrons. *Journal of Non-Crystalline Solids*, 246, pp.1-8.

Guigo, N., and Sbirrazzuoli, N., 2018. Thermal analysis of biobased polymers and composites. In: *Handbook of Thermal Analysis and Calorimetry*. Vol. 6. Elsevier, Netherlands, pp.399-429.

Hobbs, L.W., 1987. Electron-beam sensitivity in inorganic specimens. *Ultramicroscopy*, 23, pp.339-344.

Hofmann, M., Weigel, C., Strehle, S., and Holz, M., 2023. A *Paradigm Change: Focused Electron Beam Nanostructuring of Glas*s. Research Square, North Carolina.

Jbara, O., Cazaux, J., and Trebbia, P., 1995. Sodium diffusion in glasses during electron irradiation. *Journal of Applied Physics*, 78, pp.868-875.

Jencic, I., Bench, M.W., Robertson, I.M., and Kirk, M.A., 1995. Electron-beam-induced crystallization of isolated amorphous regions in Si, Ge, GaP, and GaAs. *Journal of Applied Physics*, 78(2), pp.974-982.

Jiang, N., Hembree, G.G., Spence, J.C.H., Qiu, J., Garcia de Abajo, F.J., and Silcox, J., 2003. Nanoring formation by direct-write inorganic electron-beam lithography. *Applied Physics Letters*, 83(3), pp.551-553.

Jiang, N., Qiu, J., and Silcox, J., 2004. Effects of high-energy electron irradiation on heavy-metal fluoride glass. *Journal of Applied Physics*, 96(11), pp.6230-6233.

Jiang, N., Qiu, J., and Spence, J.C.H., 2005. Precipitation of Ge nanoparticles from $GeO_2$ glasses in transmission electron microscope. *Applied Physics Letter*, 86, pp.143112-142113.

Jiang, N., Qiu, J., Ellison, A., and Silcox, J., 2003. Fundamentals of high-energy electron-irradiation-induced modifications of silicate glasses. *Physical Review B*, 68(6), pp.064207.

Jiang, Y.Z., Zhang, J.D., Wang, Z.J., Sun, Z., Deng, W.M., Zhao, Y.J., Lv, P., Zhang, L.M., Wang, T.S., and Chen, L., 2023. Composition dependence of element depth profiles in electron irradiated borosilicate glasses. *Journal of Non-Crystalline Solids*, 600, pp.121995.

Klimenkov, M., Matz, W., Nepjiko, S.A., and Lehmann, M., 2001. Crystallization of Ge nanoclusters in $SiO_2$ caused by electron irradiation in TEM. *Nuclear Instruments and Methods in Physics Research B*, 179, pp.209-214.

Leay, L., and Harrison, M.T., 2019. Bubble formation in nuclear glasses: A review. *Journal of Materials Research*, 34, pp.905-920.

Li, S., Zhong, J., Cui, Z., Zhang, Q., Sun, M., and Wang, Y., 2019. Electron beam-induced morphology transformations of $Fe_2TiO_5$ nanoparticles. *Journal of Materials Chemistry C*, 7, pp.13829-13838.

Liu, M., Xu, L., and Lin, X., 1994. Heating effect of electron beam bombardment. *The Journal of Scanning Microscopies*, 16(1), pp.1-5.

Liu, Z.Q., Hashimoto, H., Song, M., Mitsuishi, K., and Furuya, K., 2004. Phase transformation from $Fe_4N$ to $Fe_3O_4$ due to electron irradiation in the transmission electron microscope. *Acta Materialia*, 52, pp.1669-1674.

Mackovic, M., Niekiel, F., Wondraczek, L., and Spiecker., 2014. Direct observation of electron-beam-induced densification and hardening of silica nanoballs by *in situ* transmission electron microscopy and finite element method simulations. *Acta Materialia*, 79, pp.363-373.

Marks, L.D., Ajayan, P.M., and Dundurs, J., 1986. Quasi-melting of small particles. *Ultramicroscopy*, 20, pp.77-82.

Martinez, I.G.G., Bachmatiuk, A., Bezugly, V., Kunstmann, J., Gemming, T., Liu, Z., Guniberti, G., and Rummeli, M.H., 2016. Electron-beam induced synthesis of nanostructures: A review. *Nanoscale*, 8, pp.11340-11362.

Mauro, J.C., Ellison, A.J., and Pye, L.D., 2013. Glass: The nanotechnology connection. *International Journal of Applied Glass Science*, 4(2), pp.64-75.

Mayr, S.G., Ashkenazy, Y., Albe, K., and Averback, R.S., 2003. Mechanisms of radiation-induced viscous flow: Role of point defects. *Physical Review Letters*, 90, pp.055505.

Mohammad, A., Al-Ahmari, A.M., AlFaify, A., and Mohammed, M.K., 2016. Effect of melt parameters on density and surface roughness in electron beam melting of gamma titanium aluminide alloy. *Rapid Prototyping Journal*, 23(3), pp.474-485.

Musterman, E.J., Dierolf, V., and Jain, H., 2022. Electron beam heating as a tool for fabricating lattice engineered crystals in glass. *Optical Materials Express*, 12(8), pp.3248-3261.

Ollier, N., Rizza, G., Boizot, B., and Petite, G., 2006. Effects of temperature and flux on oxygen bubble formation in Li borosilicate glass under electron beam irradiation. *Journal of Applied Physics*, 99, pp.073511.

Qiu, J., Shirai, M., Nakaya, T., Si, J., Jiang, X., Zhu, C., and Hirao, K., 2002. Space-selective precipitation of metal nanoparticles inside glasses. *Applied Physics Letters*, 81(16), pp.3040-3042.

Rao, N.R., Rao, T.V., Rao, B.S., and Shanmukhi, P.S.V., 2021. Electron beam irradiation modification on chemical, thermal and crystalline properties of poly (L-lactic acid). *Indian Journal of Pure and Applied Physics*, 59, pp.715-722.

Rauf, I.A., 2008. Direct observation of the birth of a nanocrystalline nucleus in an amorphous matrix, *Applied Physics Letters*, 93, pp.143101-143103.

Shelby, J.E., 1980. Effect of radiation on the physical properties of borosilicate glasses. *Journal of Applied Physics*, 51, pp.2561-2565.

Shelby, J.E., 2005. *Introduction to Glass Science and Technology*. 2nd ed. New York State College of Ceramics at Alfred University School of Engineering, Alfred, NY, USA.

Shen, Y., Zhao, X., Gong, R., Ngo, E., Maurice, J.L., Cabarrocas, P.R., and Chen, W., 2022. Influence of the electron beam and the choice of heating membrane on the evolution of Si nanowires' morphology in *in situ* TEM. *Materials*, 15, pp.5244.

Sidorov, A.I., Kirpichenko, D.A., Yurina, U.V., and Podsvirov, O.A., 2021. Structural changes *in silica* glass under the action of electron beam irradiation: The effect of irradiation dose. *Glass Physics and Chemistry*, 47(2), pp.118-125.

Sigle, W., 2005. Analytical transmission electron microscopy. *Annual Review of Materials Research*, 35, pp.239-314.

Singh, S.P., and Karmakar, B., 2011. *In situ* electron beam irradiated rapid growth of bismuth nanoparticles in bismuth-based glass dielectrics at room temperature. *Journal of Nanoparticle Research*, 13, pp.3599-3606.

Skuja, L., Hirano, M., Hosono, H., and Kajihara, K., 2005. Defects in oxide glasses. *Physica Status Solidi*, 2(1), pp.15-24.

Sun, K., Wang, L.M., Ewing, R.C., and Weber, W.J., 2004. Electron irradiation induced phase separation in a sodium borosilicate glass. *Nuclear Instruments and Methods in Physics Research B*, 218, pp.368-374.

Ugurlu, O., Haus, J., Gunawan, A.A., Thomas, M.G., Maheshwari, S., Tsapatsis, M., and Mkhoyan, K.A., 2011. Radiolysis to Knock-on damage transition in zeolites under electron beam irradiation. *Physical Review B*, 83, pp.113408.

We, X., Varshneya, A.K., and Dieckmann, R., 2011. Sodium tracer diffusion in glasses of the type $(Na_2O)_{0.2}(B_2O_3)_y(SiO_2)_{0.8-y}$. *Journal of Non-Crystalline Solids*, 357, pp.3661-3669.

Weber, W.J., Ewing, R.C., Angell, C.A., Arnold, G.W., Cormack, A.N., Delaye, J.M., Griscom, D.L., Hobbs, L.W., Navrotsky, A., Price, D.L., Stoneham, A.M., and Weinberg, M.C., 1997. Radiation effects in glasses used for immobilization of high-level waste and plutonium disposition. *Journal of Materials Research*, 12, pp.1946-1978.

Yoshida, N., and Tanaka, K., 1997. Ag migration in Ag-As-S glasses induced by electron-beam irradiation. *Journal of Non-Crystalline Solids*, 210, pp.119-129.

Zheng, K., Wang, C., Cheng, Y.Q., Yue, Y., Han, X., Zhang, Z., Shan, Z., Mao, S.X., Ye, M., Yin, Y., and Ma, E., 2010. Electron-beam-assisted superplastic shaping of nanoscale amorphous silica. *Nature Communications*, 1(24), pp.1-8.